Journal of Integrative Neuroscience

J. Integr. Neurosci. **2024**; 23(3): 61
https://doi.org/10.31083/j.jin2303061

Original Research

Tanshinone IIA Regulates Synaptic Plasticity in Mg^{2+}-Free-Induced Epileptic Hippocampal Neurons via the PI3K/Akt Signaling Pathway

Meile Ma[1,†], Xi Hua[2,†], Chen Jia[3], Nan Xiao[1], Li Zhang[1], Liming Wei[3], Haisheng Jiao[3,*]

[1]College of Pharmacy, Lanzhou University, 730000 Lanzhou, Gansu, China
[2]Department of Pharmacy, Fengcheng Hospital of Shanghai Ninth People's Hospital Group, 201411 Shanghai, China
[3]Department of Pharmacy, Lanzhou University Second Hospital, 730030 Lanzhou, Gansu, China
*Correspondence: haisjiao@163.com (Haisheng Jiao)
[†]These authors contributed equally.

Academic Editors: Pablo Bascunana Almarcha and Gernot Riedel
Submitted: 1 September 2023 Revised: 17 November 2023 Accepted: 24 November 2023 Published: 19 March 2024

Abstract

Background: Tanshinone IIA (TSIIA) is an element of the effective ingredients of *Salvia miltiorrhiza* Bunge (Labiatae), exhibits a significant therapeutic effect in brain neuroprotection. The focus of this study was the examination of synaptic plasticity of in Mg^{2+}-free-induced epileptic hippocampus neurons and how TSIIA protects against it. **Methods**: The purity of the primary hippocampal neurons extracted from Sprague Dawley rats was assessed within 24 hours by microtubule-associated protein (MAP2) immunofluorescence staining. A hippocampal neuron model for Mg^{2+}-free-induced spontaneous recurrent epileptiform discharge was developed, five experimental groups were then randomized: blank (Blank), model (Model), TSIIA (TSIIA, 20 µM), LY294002 (LY294002, 25 µM), and TSIIA+LY294002 (TSIIA+LY294002, 20 µM+25 µM). FIJI software was used to examine variations of neurite complexity, total length of hippocampal neurons, number of primary dendrites and density of dendritic spines. Developmental regulation brain protein (Drebrin) and brain-derived neurotrophic factor (BDNF) expression was evaluated using immunofluorescence staining and the relative expression of phospho-protein kinase B (p-Akt)/Akt, BDNF, synaptophysin (SYN) and postsynaptic density 95 (PSD-95) determined by Western blot. **Results**: In contrast to the model group, TSIIA drastically reduced damage to synaptic plasticity of hippocampal neurons caused by epilepsy ($p < 0.05$). The TSIIA group showed a significant increase in the relative expression of PSD-95, SYN, BDNF, and p-Akt/Akt ($p < 0.01$). **Conclusions**: TSIIA was effective in reducing harm to the synaptic plasticity of hippocampal neurons induced by persistent status epilepticus, with the possible mechanism being regulation of the phosphatidylinositol 3-kinase 56 (PI3K)/Akt signaling pathway.

Keywords: epilepsy; hippocampal neurons; synaptic plasticity; TSIIA; SYN; PSD-95

1. Introduction

Among the most prevalent severe brain diseases, epilepsy is characterized by recurrent, spontaneous seizures that are the result of hypersynchronous neuronal discharge [1]. As the fourth most common neurological disorder, it impacts over 70 million people worldwide [2]. More than 20 antiepileptic drugs, such as valproate, lamotrigine, carbamazepine, phenytoin and levetiracetam [3], are available as first-line treatments for epilepsy patients, but seizure control is not achieved in approximately one-third of patients [4]. The pathogenesis of epilepsy is complicated and diverse, involving a variety of factors such as signaling transduction, ion channels, inflammatory responses [5–7], synaptic transmission, gap junctions and the immunological system [8]. Therefore, the underlying causes of epilepsy and its potential therapies are extremely rewarding research areas.

Chinese herbal remedies have had considerable success in the treatment of epileptic seizures and easing side effects associated with antiepileptic drugs. Natural plants are used to obtain or synthesize traditional Chinese herbal medicines. Tanshinone IIA (TSIIA) is an active component derived from *Salvia miltiorrhiza* Bunge and exhibits multiple pharmacological properties, including antiatherosclerosis, anti-cancer, anti-inflammation, antioxidation, anti-tumor, cardioprotection, neuroprotection, renoprotection and hepatoprotection [9–11]. Recently, research into TSIIA on neuroprotection has grown substantially. A study by Lin *et al.* [12] has shown that TSIIA ameliorated the learning and memory deficits caused by Ab1-42 in rats with mechanisms involving the extracellular signal-regulated protein kinase (ERK) and glycogen synthase kinase-3b (GSK-3β) signal pathway. Ma *et al.* [13] have shown that a TSIIA microemulsion has neuroprotective effects against cerebral ischemia-reperfusion damage via controlling h3k18ac and h4k8ac. Li *et al.* [14] demonstrated that TSIIA exerts neuroprotective effects through energizing the cannabinoid receptor 1 (CNR1)/phosphatidylinositol 3-kinase (PI3K)/protein kinase B (AKT) signaling pathway to antagonize hippocampal apoptosis and ameliorate sleep-deprivation-induced impairments in spatial recognition and learning memory in rats. Moreover, TSIIA has also been reported by the authors to have antiepileptic and cognitive function-improving

Copyright: © 2024 The Author(s). Published by IMR Press.
This is an open access article under the CC BY 4.0 license.

Publisher's Note: IMR Press stays neutral with regard to jurisdictional claims in published maps and institutional affiliations.

properties, which are principally mediated through modulating synaptic plasticity [15].

The modification of neuronal connection strength which depends on activities, namely synaptic plasticity, is widely acknowledged as a crucial component of learning and memory [16]. The network functions of the brain are facilitated by the interaction of different types of synaptic plasticity [17,18]. Furthermore, a variety of neurological and neuropsychiatric conditions, including Alzheimers, schizophrenia and epilepsy are accompanied by impairments in synaptic plasticity [15,19]. Persistent status epilepticus or recurrent seizures can alter brain tissue, in particular the shape and function of the hippocampus, and damage synaptic plasticity in hippocampal neurons [20]. Consequently, understanding the mechanisms behind alterations in synaptic plasticity is crucial to the treatment of epilepsy.

Mg^{2+}-free-induced epileptic hippocampal neuron models have been established to assess TSIIA's efficacy on epileptic synaptic plasticity and its mechanism of action. Our study based on the above model demonstrated that TSIIA ameliorates epilepsy-induced synaptic plasticity impairment, and that the PI3K/Akt signaling pathway may be implicated in the aforementioned process. This research offers new perspectives and a conceptual foundation for the investigation of TSIIA's pharmacological effects on epilepsy and the process of synaptic plasticity.

2. Materials and Methods

2.1 Animals

Hippocampal neurons isolated from the brains of newborn Sprague-Dawley rats within 24 hours, purchased from Lanzhou University's GLP Experimental Center (Lanzhou, Gansu, China) were used in this study. The Institutional Animal Care and Animal Ethics Committee of Lanzhou University Second Hospital authorized all experimental animal operations and sample collection (approval number: D2021-051).

2.2 Cultures of Primary Hippocampal Neurons

Rats were decapitated and their brains were dissected out and separated for the preparation of primary hippocampal neurons. 0.25% trypsin digestion solution (meilunbio, Dalian, Liaoning, China, Cat# MA0234-Apr-26F) was used to digest the hippocampal tissue for 15 minutes at 37 °C. To stop the digestion and convert it into a single-cell suspension, an equivalent amount of pre-cooled growing medium was added. This medium comprised three ingredients: Dulbecco's Modified Eagle Medium/Nutrient Mixture F-12 (DMEM/F12) (Shanghai Basalmedia Technologies Co., Ltd., Shanghai, China, Cat# K210815), fetal bovine serum (meilunbio, Cat# O0201A) and penicillin/streptomycin (100×, meilunbio, China, Cat# MA0110) in the proportion 89:10:1. Cells in the neurobasal media were then centrifuged to remove trypsin and cell debris. Cells were counted under a microscope and then cultivated at a density of 1.0×10^5/mL on glass coverslips (18 mm diameter) pre-coated with poly-L-lysine (10×, Solarbio, Beijing, China, Cat# 20200927) in a cell incubator with 5% carbon dioxide (CO_2) and 95% air at 37 °C. Five hours into the initial inoculation phase, the medium was changed to a maintenance medium devoid of serum. The maintenance medium was composed of DMEM/F12, B27 Supplement (50×, Gibco, Grand Island, NY, USA, Cat# 2234247), L-glutamine (100×, Solarbio, Cat# G0200) and penicillin/streptomycin in the ratio of 387:8:1:4, which inhibited growth and survival of glial cells and 50% of the maintenance medium was changed every three days. Cell growth status, morphology and density were observed and noted during cultivation.

2.3 Identification and Purity Analysis of Primary Hippocampal Neurons

Rat hippocampal neurons were cultured *in vitro* for seven days before fixation for 20 minutes with 4% paraformaldehyde (meilunbio, Cat# MA0192-Mar-23G) and permeabilization for 10 minutes with 0.3% Triton X-100 (Solarbio, Cat# T8200). Neurons were probed with 1:100 diluted anti-microtubule-associated protein 2 (MAP2; 1:100 dilution; ABclonal Biotechnology Co., Ltd., Wuhan, Hubei, China, Cat# 3560640007) stored overnight in a 4 °C refrigerator after blocking with 5% bovine serum albumin (Solarbio, China, Cat# 20210326) for 25 minutes at ambient temperature. The secondary antibody Dylight 488-goat anti-rabbit IgG (1:100; Boster Biological Technology Co., Ltd., Wuhan, Hubei, China, Cat# BST14B25C27) was then dark applied to the cells for an hour at room temperature. 4,6-diamino-2-phenyl indole (DAPI, Boster Biological Technology Co., Ltd., Cat# 15F03A76) was used to restain the nuclei for 15 minutes. Sections were then sealed using a fluorescence-quenching sealer (Boster Biological Technology Co., Ltd., Cat# 14E07A09). To identify neurons, fluorescence signals were observed using an ortho-fluorescence microscope (Olymus, Tokyo, Japan, Cat# BX53+DP74). To calculate the percentage purity of hippocampal neurons, the microtubule-associated protein (MAP2)-positive cell count was divided by the DAPI-positive cell count yields of hippocampal neurons in five randomly selected fields of vision at a magnification of 200×.

A neuron-specific microtubule-associated protein called MAP2 is expressed in both adult and immature hippocampal neurons, making it possible to distinguish neurons [21]. The purity of hippocampal neurons was greater than 95% and sufficient for the subsequent experiments. Results of immunofluorescence staining identification are shown as 98% in Fig. 1.

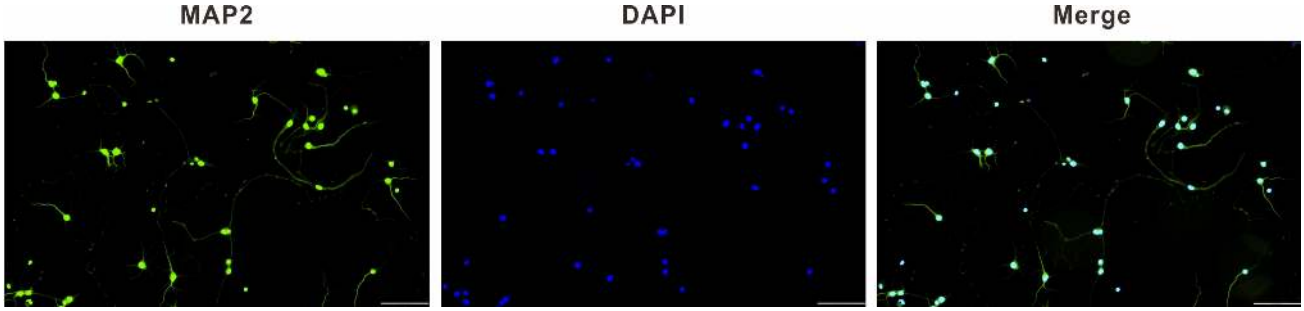


Fig. 1. MAP2 immunofluorescence identification of primary hippocampal neurons (×200), scale bar: 100 μm. MAP2, microtubule-associated protein; DAPI, 4,6-diamino-2-phenyl indole.

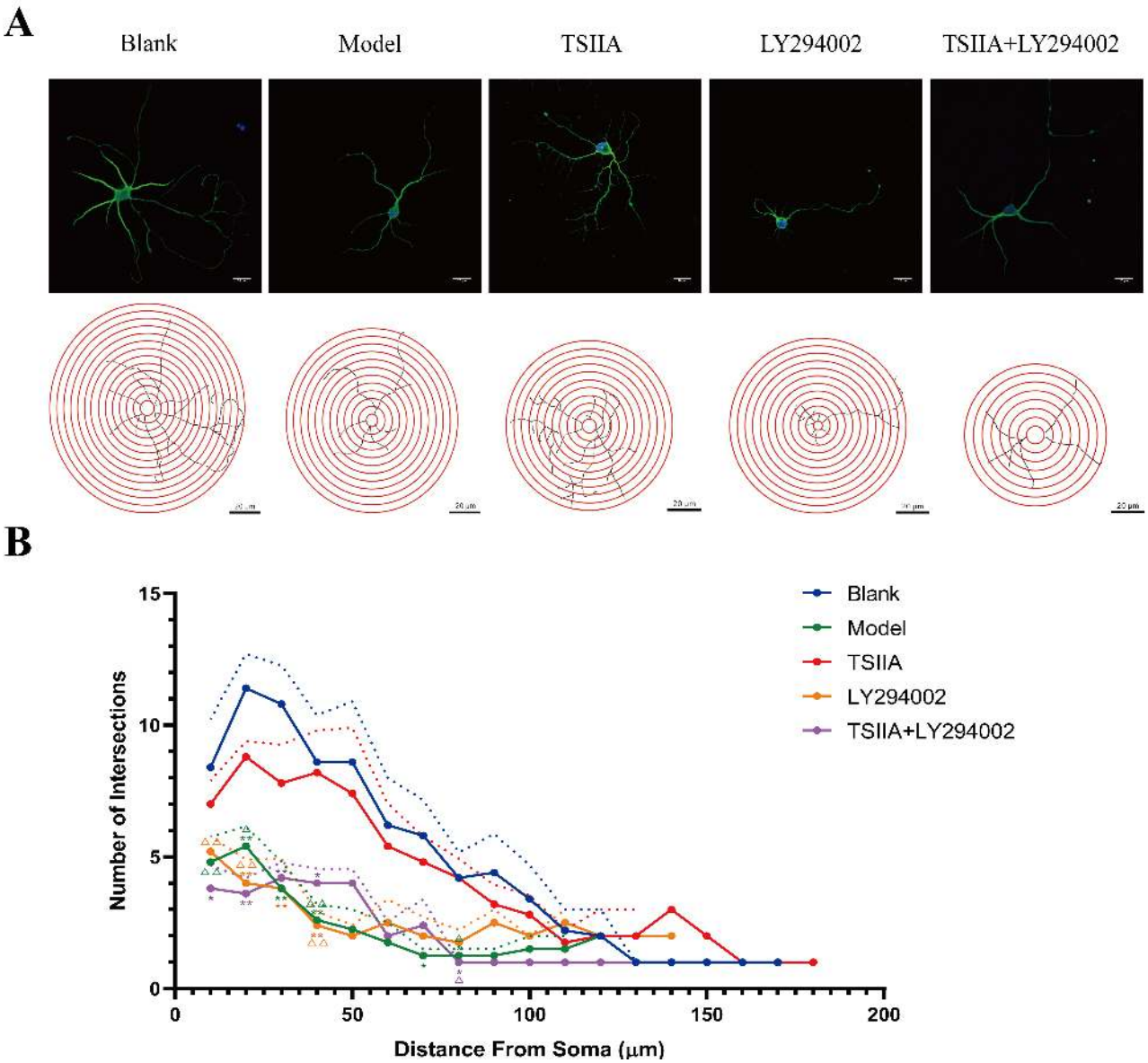


Fig. 2. Effect of TSIIA on protrusion complexity. (A) Cytoskeleton and protrusion trajectory of hippocampal neurons in each group (magnification ×630), scale bar: 20 μm. (B) Statistical plots of the intersections' number of hippocampal neuronal protrusions within concentric circles. $^{*}p < 0.05$, $^{**}p < 0.01$ vs. Blank group; $^{\triangle}p < 0.05$, $^{\triangle\triangle}p < 0.01$ vs. TSIIA group (n = 5 per group). TSIIA, Tanshinone IIA.

Table 1. Results on the number of intersections of hippocampal neuronal cell protrusions with concentric circles.

Distance from soma	Blank	Model	TSIIA	LY294002	TSIIA+LY294002
10	8.40 ± 1.64	4.80 ± 0.87$^{\triangle\triangle}$	7.00 ± 0.80$^{\triangle\triangle}$	5.20 ± 0.52	3.80 ± 0.77*
20	11.40 ± 1.15	5.40 ± 0.67$^{**,\triangle}$	8.80 ± 0.52	4.00 ± 0.80$^{**,\triangle\triangle}$	3.60 ± 0.54$^{**,\triangle\triangle}$
30	10.80 ± 1.31	3.80 ± 0.91**	7.80 ± 1.31	3.80 ± 1.00**	4.20 ± 0.52**
40	8.60 ± 1.59	2.60 ± 0.54$^{**,\triangle\triangle}$	8.20 ± 1.43	2.40 ± 0.46$^{**,\triangle\triangle}$	4.00 ± 0.49*
50	8.60 ± 2.05	2.25 ± 0.65	7.40 ± 2.24	2.00 ± 0.35	4.00 ± 0.49
60	6.20 ± 1.61	1.75 ± 0.65	5.40 ± 1.46	2.50 ± 0.75	2.00 ± 0.49
70	5.80 ± 1.21	1.25 ± 0.22*	4.80 ± 0.87	2.00 ± 0.61	2.40 ± 0.88
80	4.20 ± 0.87	1.25 ± 0.22$^{*,\triangle}$	4.20 ± 0.66	1.75 ± 0.41	1.00 ± 0.00$^{*,\triangle}$
90	4.40 ± 1.31	1.25 ± 0.22	3.20 ± 0.66	2.50 ± 0.35	1.00 ± 0.00
100	3.40 ± 1.15	1.50 ± 0.35	2.80 ± 0.66	2.00 ± 0.00	1.00 ± 0.00
110	2.20 ± 0.72	1.50 ± 0.35	1.75 ± 0.41	2.50 ± 0.35	1.00 ± 0.00
120	2.00 ± 0.87	2.00 ± 0.00	2.00 ± 0.71	2.00 ± 0.00	1.00 ± 0.00
130	1.00 ± 0.00	1.00 ± 0.00	2.00 ± 0.71	2.00 ± 0.00	1.00 ± 0.00
140	1.00 ± 0.00	1.00 ± 0.00	3.00 ± 0.00	2.00 ± 0.00	1.00 ± 0.00
150	1.00 ± 0.00	1.00 ± 0.00	2.00 ± 0.00		1.00 ± 0.00
160	1.00 ± 0.00	1.00 ± 0.00	1.00 ± 0.00		1.00 ± 0.00
170	1.00 ± 0.00		1.00 ± 0.00		
180			1.00 ± 0.00		

Results are presented as mean ± SEM (standard error of the mean).

$^{*}p < 0.05$, ** $p < 0.01$ vs. Blank group; $^{\triangle}p < 0.05$, $^{\triangle\triangle}p < 0.01$ vs. TSIIA group (n = 5 per group).

2.4 Drugs Treatment

Five groups of primary hippocampal neurons were selected at random: blank (Blank), model (Model), TSIIA (TSIIA, 20 μM), LY294002 (LY294002, 25 μM), and TSIIA+LY294002 (TSIIA+LY294002, 20 μM+25 μM). At nine days *in vitro*, the Blank group was added to the normal medium, and the other groups received additions of the magnesium-free external solution [22–24]. The above solutions were switched to a maintenance medium after three hours, and the maintenance medium of the drug groups was supplemented respectively with the corresponding concentrations of 20 μM TSIIA (Shanghai Yuanye Bio-Technology Co., Ltd., Shanghai, China, Cat# Y14M10C82864), 25 μM LY294002 (MedChemExpress LLC, Monmouth Junction, NJ, USA, Cat# 51598) and a combination of 20 μM TSIIA and 25 μM LY294002, and then incubated for further 24 hours.

2.5 Double Immunofluorescent Staining

Hippocampal neurons in each group were permeabilized with 0.3% Triton X-100 after being exposed to 4% paraformaldehyde. The cells were then treated with 5% Bovine serum albumin (BSA) for 25 minutes to block them, before being incubated overnight with a primary antibody mixture consisting of MAP2, developmental regulation brain protein (Drebrin) (Santa Cruz Biotechnology, Dallas, TX, USA, Cat# B6535), 5% BSA and Phosphate Buffered Saline (PBS) in a ratio of 1:1:20:80, and then with a secondary antibody mixture consisting of Dylight 488-goat anti-rabbit IgG, Cy3-goat anti-mouse IgG (Boster Biological Technology Co., Ltd., China, Cat# BST16A25C16F31) and 5% BSA and PBS in a ratio of 1:1:20:80 for one hour. The nuclei were sealed with an anti-fluorescence blocker after a PBS rinse and 15 minutes of DAPI staining. Hippocampal neurons were examined and photographed utilizing a two-photon confocal laser scanning microscope (Carl Zeiss, Oberkochen, Bartenburg, Germany, Cat# Zeiss LSM880). Variations in neurite complexity, total length of hippocampal neurons, number of primary dendrites, and density of dendritic spines were analyzed using FIJI software (Version 2.9.0, National Institutes of Health, Bethesda, MD, USA). The average fluorescence density of each group of Drebrin treated neurons was calculated using Image J software (Version 1.52p, National Institutes of Health).

2.6 BDNF Immunofluorescent Staining

Immunofluorescence staining was carried out at nine days *in vitro* to detect neurons using brain-derived neurotrophic factor (BDNF) antibody (1:100, ABclonal Biotechnology Co., Ltd., China, Cat# 3507522015), and DAPI was used to count all cells in the culture. Photographs were taken at a magnification of 200× magnification in five randomly selected areas, and Image J was used to calculate the average fluorescence density of each group of BDNF.

2.7 Western Blot Analysis

Following their individual treatments, neurons were cleaved by using a cell lysis buffer, containing radioimmunoprecipitation assay buffer, phenylmethanesulfonyl fluoride and Phosphatase inhibitor cocktail I in a 98:1:1 ratio, to extract total protein, followed by Bicinchoninic acid (BCA) Protein Assay Kit (Solarbio, China, Cat# PC0020)

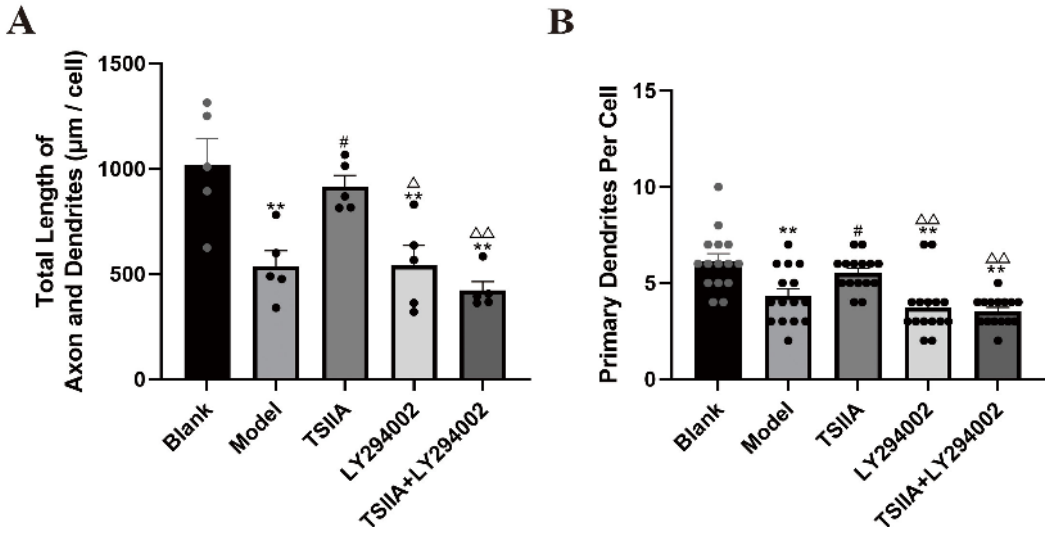


Fig. 3. Total length and the primary dendrites count of hippocampal neuron protrusions in each group. (A) The total length of hippocampal neuron protrusions in each group. $^{**}p < 0.01$ vs. Blank group; $^{\#}p < 0.05$ vs. Model group; $^{\triangle}p < 0.05$, $^{\triangle\triangle}p < 0.01$ vs. TSIIA group (n = 5 per group). (B) The primary dendrites count on hippocampal neurons in each group. $^{**}p < 0.01$ vs. Blank group; $^{\#}p < 0.05$ vs. Model group; $^{\triangle\triangle}p < 0.01$ vs. TSIIA group (n = 15 dendrites per group).

to detect protein concentration. To denature the proteins, all samples were mixed with 5× loading buffer and boiled. After electrophoretic separation of total proteins using 10% sodium dodecyl sulfate-polyacrylamide gel electrophoresis (SDS-PAGE) gels, total protein was then transferred to polyvinylidene difluoride membranes (0.22 μm, Solarbio, China, Cat# YA1701), at room temperature. Blocking was done for 1.5 hours using 5% skim milk powder added with Tris Buffered Saline with Tween 20 (TBST), a mixture solution of Tris-buffered saline and 0.1% Tween-20 (Solarbio, China, Cat# 626NO45), and then the following primary antibodies were incubated at 4 °C overnight: phospho-protein kinase B (p-Akt) antibody (1:800, ABclonal Biotechnology Co., Ltd., China, Cat# 21155950401), Akt 1/2/3 antibody (1:1000, Boster Biological Technology Co., Ltd., China, Cat# BST17614400), SYN antibody (1:1000, ABclonal Biotechnology Co., Ltd., China, Cat#3561324106), BDNF antibody, PSD-95 antibody (1:1000, Boster Biological Technology Co., Ltd., China, Cat# M02128-1), and GAPDH antibody (1:2000, Sangon Biotech, Shanghai, China, Cat# B661204-0001). Next, membranes were cleaned with TBST for 4 × 8 minutes, and the appropriate secondary antibody was then applied for two hours. Grayscale values of each protein on the protein strip were examined using Image J software after protein strips were scanned using Enhanced Chemiluminescence (ECL) luminescence imaging.

2.8 Statistical Analysis

GraphPad Prism 8.0.1 (GraphPad Software, San Diego, CA, USA) and SPSS Statistics 25.0 (IBM Corp., Armonk, NY, USA) were used to evaluate the obtained data, which were expressed as $x \pm$ SEM (standard error of the mean). A one-way analysis of variance was used to compare groups. Value of either $p < 0.05$ or $p < 0.01$ were regarded as statistically significant.

3. Results

3.1 Effect of TSIIA on Protrusion Complexity of Hippocampal Neurons

FIJI software was used to examine the morphology of neurons to assess the state of neuronal protrusions (Fig. 2A). After intervention with a magnesium-free external solution, the protrusions and branches of the hippocampal neurons in each experimental group were smaller and thicker than those in the Blank group, and some were beaded. Sholl analysis was used to compare the complexity of protrusions in each group (Fig. 2B, Table 1). Only the TSIIA+LY294002 group was clearly distinguishable from the Blank group ($p < 0.05$) with regard to the the intersections' number of hippocampal neuronal protrusions within concentric circles at 10 μm from the cell body; the Model, LY2940002 and TSIIA+LY294002 groups also exhibited fewer intersections than the TSIIA group, with the first two groups being statistically different ($p < 0.01$). Similarly, when compared to the Blank group, the concentric protrusion count marginally decreased in the TSIIA group, but reduction in the number of concentric protrusions was more pronounced in the other groups, as measured by later measurements of protrusion complexity per 10 μm from the cell body.

3.2 Effect of TSIIA on Total Length and Primary Dendrite Count of Hippocampal Neurons

The "Simple Neurite Tracer" in the FIJI software was used to measure the total length of neurite protrusions

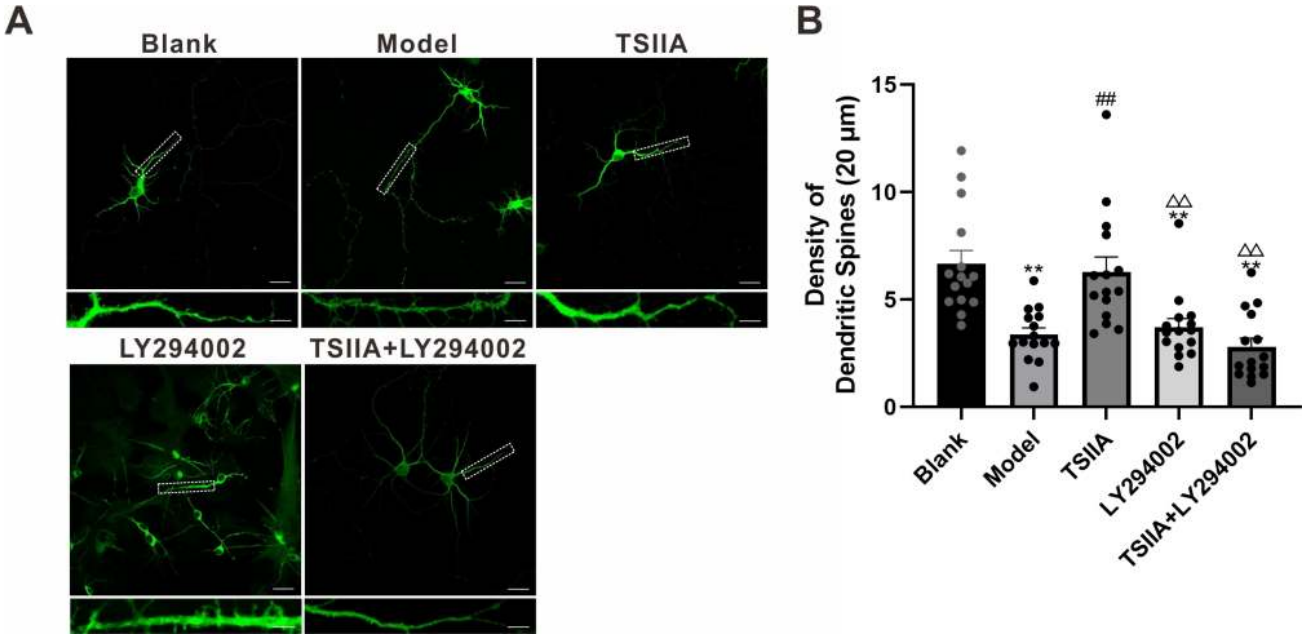


Fig. 4. Dendritic spine density of hippocampal neurons in each group. (A) Hippocampal neurons in each group were immunofluorescently stained for MAP2 (scale bar: 20 μm), and the secondary dendrites in the white dashed box were locally magnified (scale bar: 5 μm). (B) Statistics of dendritic spine density of hippocampal neurons in each group. $^{**}p < 0.01$ vs. Blank group; $^{\#\#}p < 0.01$ vs. Model group; $^{\triangle\triangle}p < 0.01$ vs. TSIIA group (n = 15 dendrites per group).

(Fig. 3A). The total protrusion length of the experimental groups decreased after intervention with the magnesium-free external solution, with significant differences among the Model, LY294002, TSIIA+LY294002 and the Blank groups ($p < 0.01$, Model 536.8 ± 73.6, LY294002 542.9 ± 93.1, TSIIA+LY294002 422.3 ± 41.0 vs. Blank 1018 ± 125.0 μm). When compared to Model, LY294002, and TSIIA+LY294002 groups (vs. Model, $p < 0.05$; vs. LY294002, $p < 0.05$; vs. TSIIA+LY294002, $p < 0.01$), the total protrusion length was enhanced by TSIIA alone (915.8 ± 52.3 μm), which was also substantially increased.

Statistical analysis of primary dendrites in each group (Fig. 3B), Model, LY294002, and TSIIA+LY294002 showed these groups all exhibited considerably fewer primary dendrites than those in the Blank group 6.13 ± 0.40 ($p < 0.01$, Model 4.33 ± 0.37, LY294002 3.73 ± 0.38, TSIIA+LY294002 3.53 ± 0.19), although the TSIIA group had 5.53 ± 0.24, which was not significantly different from the Blank group. TSIIA was significantly greater than the Model group ($p < 0.05$), whereas LY294002 and TSIIA+LY294002 were considerably decreased when compared with the TSIIA group ($p < 0.01$).

3.3 Effect of TSIIA on Dendritic Spine Density in Hippocampal Neurons

Among the dendritic spine morphologies on the secondary dendrites of hippocampal neurons in each group (Fig. 4A), the Model and LY294002 groups mostly had stubby, filopodia-shaped dendritic spines, whereas the Blank, TSIIA and TSIIA+LY294002 groups mostly had thin mushroom-shaped spines. Data (Fig. 4B) showed the dendritic spine density was significantly less in the Model, LY294002 and TSIIA+LY294002 groups than in the Blank group ($p < 0.01$, Model 3.37 ± 0.31, LY294002 3.71 ± 0.40 and TSIIA+LY294002 2.79 ± 0.40 vs. Blank 6.65 ± 0.63). When compared to the Model group, dendritic spine density was substantially greater in the TSIIA group ($p < 0.01$) and significantly decreased in the LY294002 and TSIIA+LY294002 groups when compared with the TSIIA group ($p < 0.01$) after intervention with the TSIIA medicinal solution.

3.4 Expression of Drebrin Protein in Hippocampal Neurons

Drebrin has an essential influence on the growth and development of dendritic spines. According to the findings of immunofluorescence staining (Fig. 5A), Drebrin protein was predominantly expressed in the primary dendrites and cytoplasm of hippocampal neurons, and its fluorescence intensity gradually decreased with the extension of neuronal protrusions. When the average fluorescence intensity of Drebrin protein in each group was counted (Fig. 5B), we discovered that the expression of Drebrin within the Model, LY294002 and TSIIA+LY294002 groups was significantly lower when compared to the Blank group ($p < 0.01$, Model 0.08 ± 0.02, LY294002 0.08 ± 0.01, TSIIA+LY294002 0.09 ± 0.02 vs. Blank 0.36 ± 0.04), while the TSIIA group only showed no statistically meaningful difference (TSIIA 0.25 ± 0.05 vs. Blank 0.36 ± 0.04). When compared to the Model group, the TSIIA group's Drebrin expression was

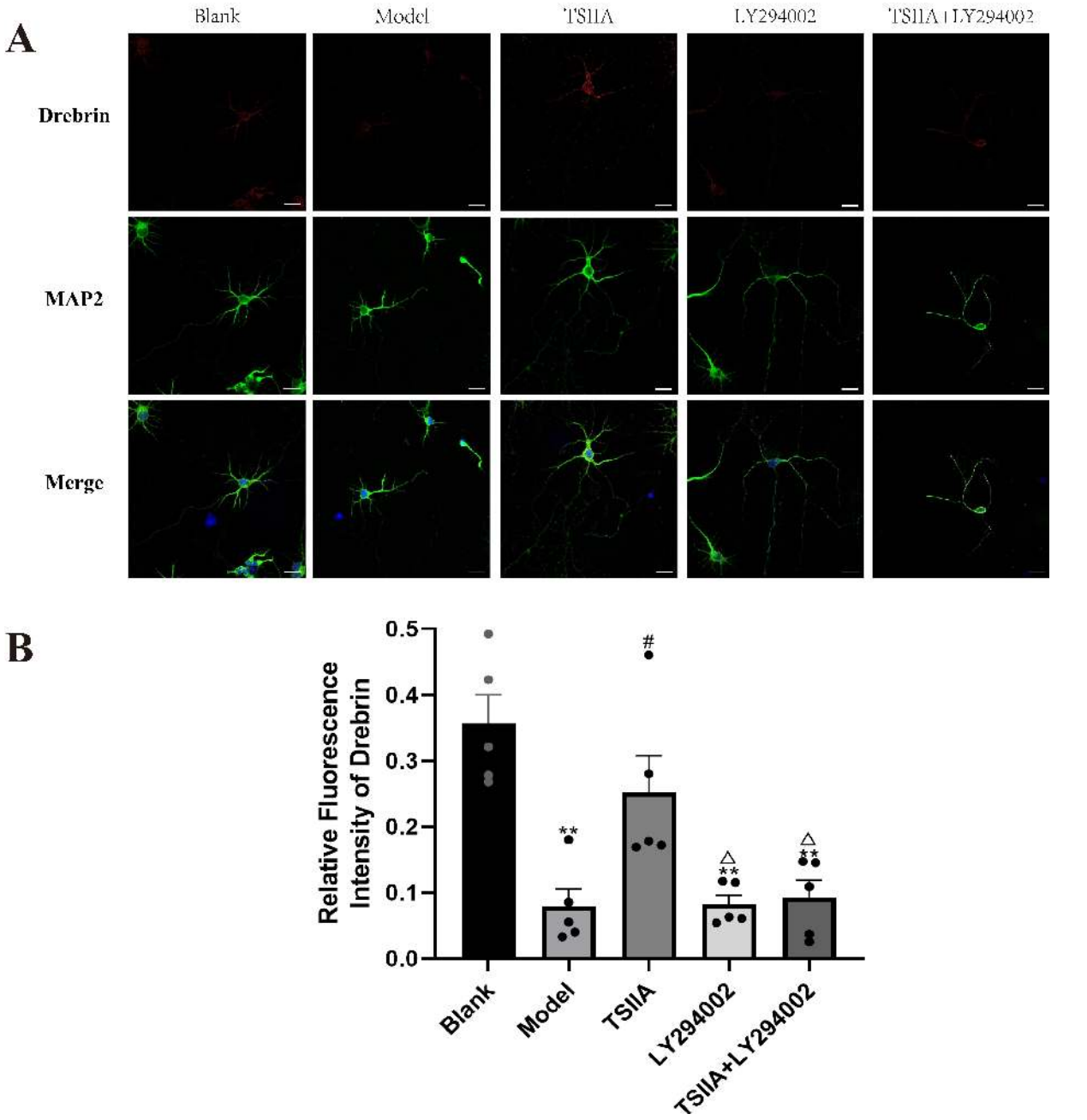


Fig. 5. Drebrin protein expression on hippocampal neurons in each group. (A) Plots of immunofluorescence staining results of Drebrin in hippocampal neurons in each group (magnification ×630), scale bar: 20 μm. (B) Statistical plots of relative fluorescence intensity of Drebrin protein in hippocampal neurons in each group. $^{**}p < 0.01$ vs. Blank group; $^{\#}p < 0.05$, vs. Model group; $^{\triangle}p < 0.05$ vs. TSIIA group (n = 5 per group). Drebrin, Developmental regulation brain protein.

significantly enhanced ($p < 0.05$). When the TSIIA group was contrasted with the LY294002 and TSIIA+LY294002 groups, there was a significant difference in Drebrin fluorescence intensity ($p < 0.05$).

3.5 Expression of BDNF in Hippocampal Neurons

Extensively expressed in the brain and nervous system, BDNF is involved in promoting neuronal processes such as axonal and dendritic growth as well as synapse formation. Immunostaining results (Fig. 6) showed that the Model, LY294002 and TSIIA+LY294002 groups had significantly lower levels of BDNF expression than the Blank group (Blank 0.98 ± 0.12 vs. Model 0.42 ± 0.09, $p < 0.05$; vs. LY294002 0.49 ± 0.09, $p < 0.05$, vs. TSIIA+LY294002 0.36 ± 0.04, $p < 0.01$), but not in the TSIIA group (1.15 ± 0.17). The BDNF protein expression was substantially increased in the TSIIA group in contrast to the Model group ($p < 0.01$), while the LY294002 and TSIIA+LY294002 groups significantly reduced when compared with the TSIIA group ($p < 0.01$).

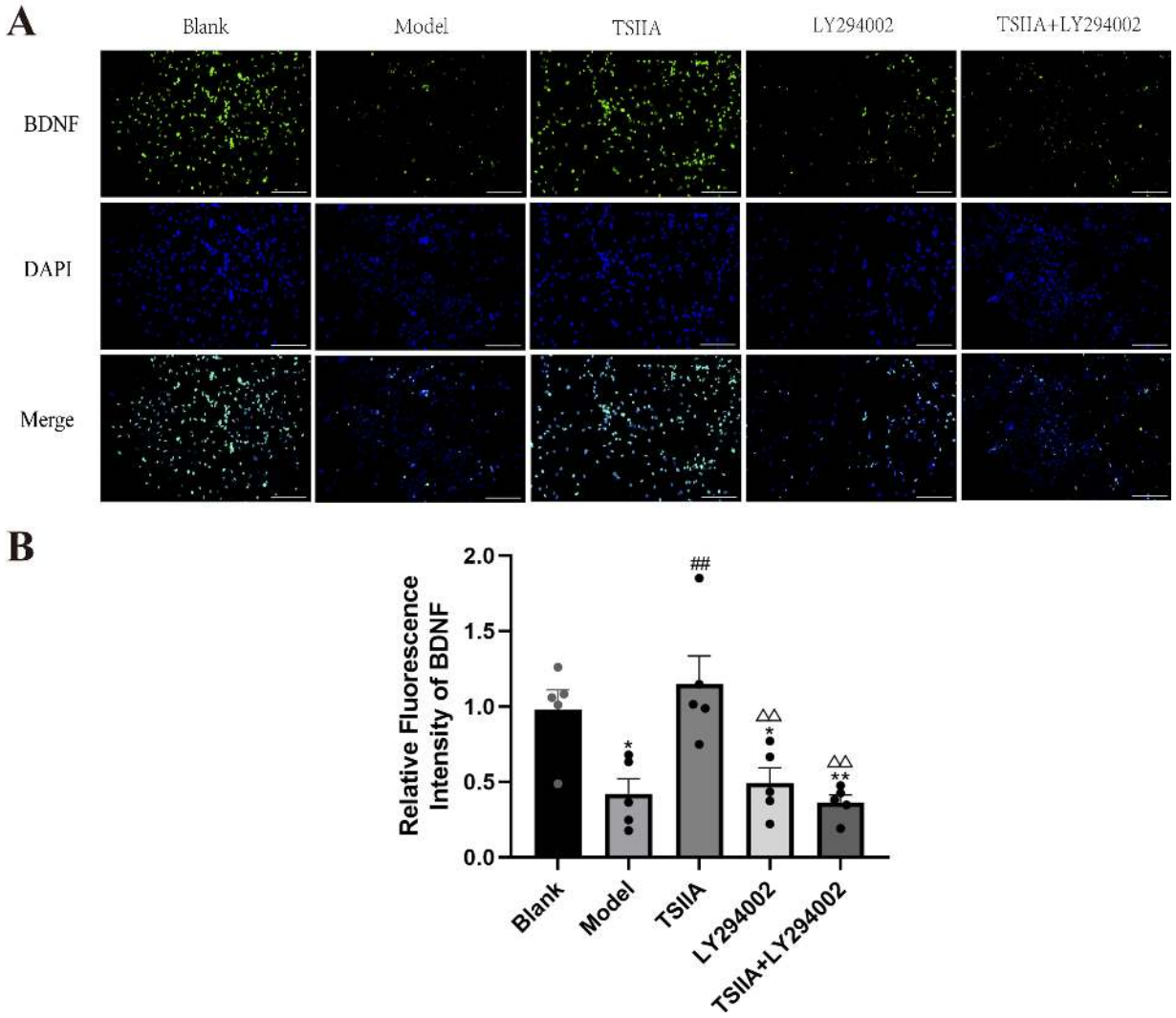


Fig. 6. Intracellular BDNF staining in hippocampal neurons. (A) Immunofluorescence staining plots of intracellular BDNF in hippocampal neurons of each group (magnification ×200), scale bar: 100 µm. (B) Statistical plots of mean fluorescence intensity of BDNF protein in hippocampal neurons of each group. $^{*}p < 0.05$, $^{**}p < 0.01$ vs. Blank group; $^{\#\#}p < 0.01$ vs. Model group; $^{\triangle\triangle}p < 0.01$ vs. TSIIA group (n = 5 per group). BDNF, Brain-derived neurotrophic factor.

3.6 Expression of BDNF, SYN, PSD-95, p-Akt and Akt Proteins in Hippocampal Neurons

The Western Blot findings are illustrated in Fig. 7A, analyzed in Fig. 7B–E and Table 2. BDNF protein expression analyzed with Image J software showed (Fig. 7B) that the expression of BDNF protein within the Model, LY294002 and TSIIA+LY294002 groups was significantly decreased ($p < 0.01$) in contrast to the Blank group, and there was no significant difference in how the TSIIA group performed. BDNF expression was significantly increased after TSIIA intervention when comparing the TSIIA group with the Model group ($p < 0.01$); when compared to the TSIIA group, BDNF protein expression was considerably reduced within the LY294002 and TSIIA+LY294002 groups ($p < 0.01$).

When assessing the biological functions of synapses, researchers frequently look at the expression levels of synaptophysin (SYN) and postsynaptic density 95 (PSD-95). Results demonstrated (Fig. 7C,D) that SYN and PSD-95 proteins expression in the Model, LY294002 and TSIIA+LY294002 groups were significantly decreased as compared to the Blank group ($p < 0.01$). SYN protein expression level was significantly raised in the TSIIA group ($p < 0.01$), but the PSD-95 protein expression level was significantly reduced ($p < 0.01$). The TSIIA group significantly outperformed the Model group in terms of SYN and PSD-95 protein expression ($p < 0.01$), while there was a dramatically higher level of PSD-95 protein expression in the LY294002 group ($p < 0.01$). Additionally, the LY294002 and TSIIA+LY294002 groups had significantly lower levels of SYN and PSD-95 protein expression than the TSIIA group ($p < 0.05$).

According to the p-Akt/Akt protein expression data results (Fig. 7E), the expression of this protein was

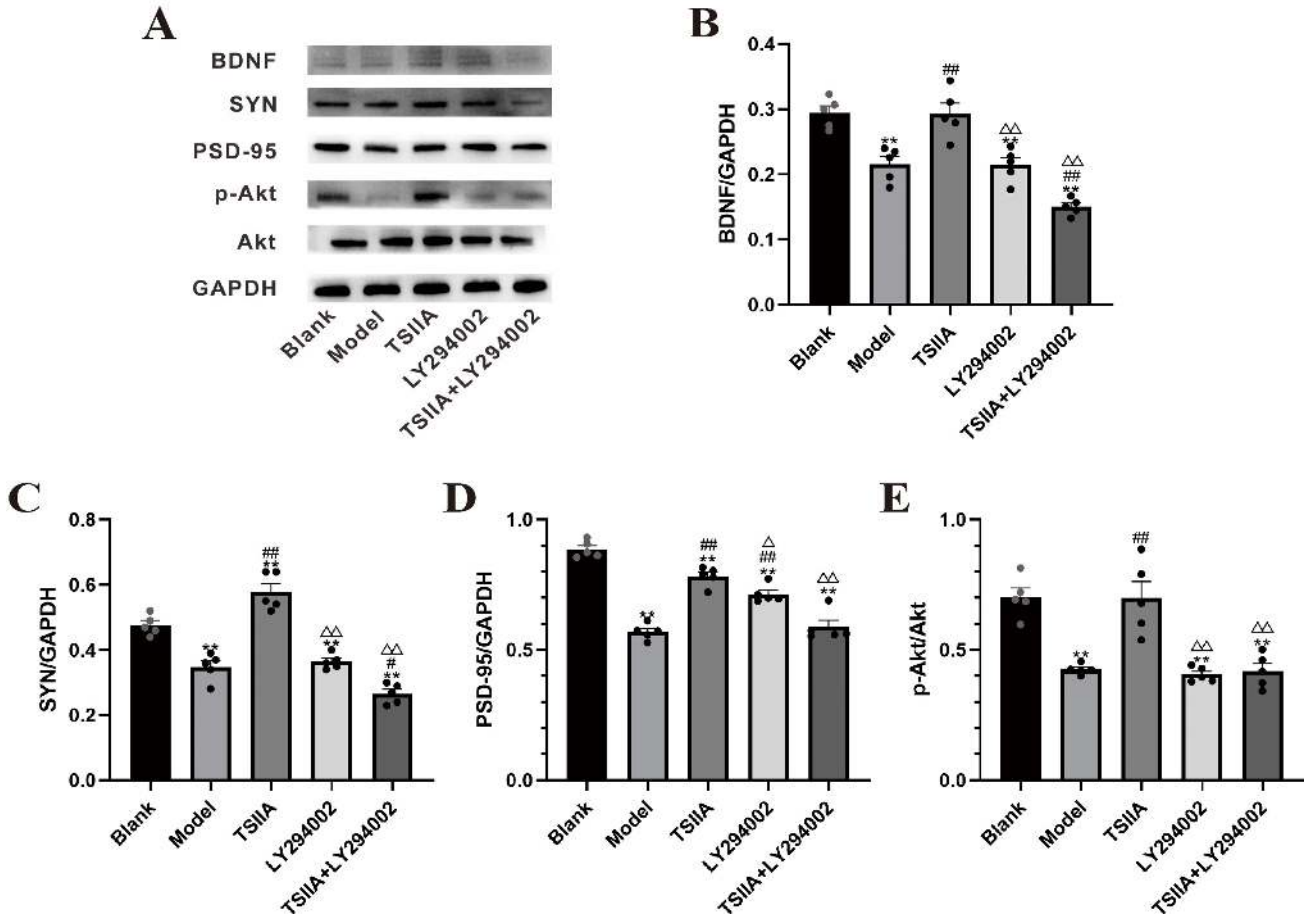


Fig. 7. Expression of BDNF, SYN, PSD-95, p-Akt and Akt proteins in each group of hippocampal neurons. (A) Western blot results of BDNF, SYN, PSD-95, p-Akt, Akt and GAPDH proteins in each group of hippocampal neuronal cells. (B–E) Relative expression of BDNF/GAPDH, SYN/GAPDH, PSD-95/GAPDH and p-Akt/Akt in each group of hippocampal neurons. $^{**}p < 0.01$ vs. Blank group; $^{\#}p < 0.05$, $^{\#\#}p < 0.01$ vs. Model group; $^{\triangle}p < 0.05$, $^{\triangle\triangle}p < 0.01$ vs. TSIIA group (n = 5 per group). BDNF, Brain-derived neurotrophic factor; SYN, synaptophysin; PSD-95, postsynaptic density 95; p-Akt, phospho-protein kinase B; Akt, protein kinase B.

significantly lower within the Model, LY294002 and TSIIA+LY294002 groups when compared to the Blank group ($p < 0.01$), while there was no statistical difference in the tanshinone IIA group. The TSIIA group significantly outperformed the Model group in terms of the relative expression of p-Akt/Akt ($p < 0.01$), whereas the LY294002 and TSIIA+LY294002 groups significantly underperformed the TSIIA group ($p < 0.01$).

4. Discussion

Treatment of neuronal cells with magnesium-free extracellular fluid for three hours resulted in convulsive cellular discharges and induced a model of spontaneous recurrent epileptiform discharge [22,24]. The persistent epileptic seizures showed morphological features of apoptosis [25,26]. In the present study, after three hours of induction of hippocampal neurons by magnesium-free extracelluar fluid, some cells floated in the medium leading to a sharp decrease in the number of hippocampal neurons, which indicates that the hippocampal neuronal epilepsy model due to this induction procedure not only alters changes in the synaptic plasticity of neurons, but also leads to apoptotic cell death.

Changing the intensity and effectiveness of synaptic transmission at pre-existing synapses in response to variations in activity is known as synaptic plasticity, which is a fundamental characteristic of neurons [27], that includes functional and structural plasticity. Changes in functional plasticity are the biological underpinning of learning and memory, whereas structural plasticity is a key mechanism for maintaining synaptic strength within a dynamic range suited for the bidirectional modulation of neuronal excitability [28]. Here, the structural plasticity of the hippocampus was investigated. When counting protrusion complexity, total protrusion length and the number of primary dendrites, it was found significant changes in the morphology of hippocampal neurons within 24 hours of culture with Mg^{2+}-free-induced epileptic modeling when compared to the Blank group. This demonstrates how seizures have a negative impact on the structural growth of

Table 2. Expression of BDNF, SYN, PSD-95, p-Akt and Akt proteins.

Proteins	Blank	Model	TSIIA	LY294002	TSIIA+LY294002
BDNF	0.29 ± 0.01	$0.22 \pm 0.01^{**}$	$0.29 \pm 0.01^{\#\#}$	$0.21 \pm 0.01^{**,\triangle\triangle}$	$0.15 \pm 0.01^{**,\#\#,\triangle\triangle}$
SYN	0.48 ± 0.01	$0.35 \pm 0.02^{**}$	$0.58 \pm 0.02^{**,\#\#}$	$0.36 \pm 0.01^{**,\triangle\triangle}$	$0.27 \pm 0.01^{**,\#,\triangle\triangle}$
PSD-95	0.89 ± 0.01	$0.57 \pm 0.01^{**}$	$0.78 \pm 0.01^{**,\#\#}$	$0.71 \pm 0.01^{**,\#\#,\triangle}$	$0.59 \pm 0.02^{**,\triangle\triangle}$
p-Akt	0.70 ± 0.03	$0.43 \pm 0.01^{**}$	$0.70 \pm 0.06^{\#\#}$	$0.41 \pm 0.01^{**,\triangle\triangle}$	$0.42 \pm 0.03^{**,\triangle\triangle}$

Results are presented as mean ± SEM.

$^{**}p < 0.01$ vs. Blank group; $^{\#}p < 0.05$, $^{\#\#}p < 0.01$ vs. Model group; $^{\triangle}p < 0.05$, $^{\triangle\triangle}p < 0.01$ vs. TSIIA group (n = 5 per group).

hippocampal neurons, which may decrease the effectiveness of synaptic communication and impair cognitive performance. Addition of TSIIA greatly reduced the structural changes in hippocampal neurons, demonstrating that TSIIA has a protective effect on the damage to the structural plasticity of epileptic hippocampal neuronal cells in an Mg^{2+}-free extracellular fluid.

Small, slender, specialized protrusions of neuronal dendrites called dendritic spines mostly exhibit excitatory synapses [29]; their morphology and density serve crucial functions in synaptic plasticity and changes in the shape and quantity of dendritic spines regularly impact synaptic growth, persistence, and plasticity in both biological and pathological circumstances [30,31]. Dendritic spines are composed of four morphologies, including thin, filopodial, mushroom and stubby rows, the latter two being the mature forms [32,33]. Hippocampal neurons with Mg^{2+}-free extracellular fluid intervention were in a state of epileptiform discharge. In the process of calculating the overall number of dendritic spines, the Model group's dendritic spines were either the thin or filopodia type and their total density was lower in relation to the Blank group, which suggests that the development of spines in the brain is affected during seizures. TSIIA ameliorates the epilepsy-induced decrease in dendritic spine density and their morphology was mostly the mushroom- or stubby-types, implying that TSIIA may counteract the damage to synaptic plasticity evoked by epilepsy.

Drebrin, a actin cytoskeletal regulator in neurons, is criucial for neurite production, synaptic plasticity, and neuronal migration [34]. BDNF is involved in an assortment of neurophysiological processes, including developmental processes, modulation of neurons, glia and synaptogenesis, neuroprotection, and control of short- and long-term synaptic interactions that affect cognitive and memory mechanisms [35]. The findings of this study demonstrated that Drebrin protein expression levels in hippocampal neurons decreased when seizures occurred and that its expression level was significantly increased by TSIIA treatment. In the case of BDNF expression levels, both immunofluorescence staining and Western blot results showed generally consistent results, indicating that TSIIA may increase the amount of BDNF expression in hippocampal neurons with abnormal discharge.

SYN and PSD-95, two synapse-associated proteins, are crucial indicators of synaptic plasticity in the brain [36,37]. As demonstrated by Western blot examination, the discharge of epileptic hippocampal neurons had a substantial impact on SYN and PSD-95 expression, illustrating that synaptic plasticity was impaired. After TSIIA intervention, their expression levels were considerably increased, which demonstrated that TSIIA may regulate SYN and PSD-95 expression to improve synaptic plasticity in epileptic hippocampal neurons.

Activation of the PI3K/Akt pathway promotes adult central neuron regeneration and maintains synaptic plasticity [38,39]. Hippocampal neuronal protrusion complexity, total protrusion length, number of primary dendrites, and dendritic spine density did not differ substantially from the Model group following the administration of LY294002 alone. Simultaneously, Drebrin, BDNF, SYN and PSD-95 expression levels tended to increase, especially PSD-95, suggesting that blockade of the PI3K/Akt signaling pathway made the Mg^{2+}-free extracellular fluid epileptogenic hippocampal neurons activate other signaling pathways for a weak protective effect against synaptic plasticity injury. When TSIIA was co-administered with LY294002, hippocampal neuron morphology, total protrusion length, number of primary dendrites and dendritic spine density did not differ substantially from those of the Model group. Strikingly, the TSIIA+LY294002 group significantly decreased at the molecular level when compared with the TSIIA group, indicating that TSIIA primarily controls the PI3K/Akt signaling pathway, which regulates the synaptic biological function of hippocampal neurons, and may be employed to preserve hippocampal neurons. In summary, TSIIA regulated the synaptic biological function of hippocampal neurons mainly via the PI3K/Akt signaling pathway and ameliorated synaptic plasticity damage by enhancing the expression levels of Drebrin, SYN, and PSD-95 proteins.

5. Conclusions

The current investigation provides support for TSIIA usage in a model of neuronal epilepsy brought on by magnesium-free extracellular fluid. By the PI3K/Akt signaling pathway, TSIIA controls the synaptic biological functions of hippocampal neurons, reduces synaptic plas-

ticity damage, and elongates the total length of axon and dendrite growth by elevating the expression levels of the Drebrin, SYN and PSD-95 proteins, all of which have unmistakable neuroprotective effects.

Abbreviations

TSIIA, tanshinone IIA; MAP2, Microtubule-associated protein2; BDNF, Brain-derived neurotrophic factor; SYN, synaptophysin; PSD-95, postsynaptic density 95; Drebrin, Developmental regulation brain protein; PI3K, phosphatidylinositol 3-kinase; Akt, protein kinase B; BCA, bicinchoninic acid; SDS-PAGE, sodium dodecyl sulfate-polyacrylamide gel electrophoresis.

Availability of Data and Materials

The datasets used and analyzed during the current study are available from the corresponding author on reasonable request.

Author Contributions

HJ designed the research study and supervised the project. MM and XH performed the research, analyzed the data, and wrote the manuscript. CJ, NX, LZ, and LW provided help and advice on experimental operations and data analyses. All authors contributed to editorial changes in the manuscript. All authors read and approved the final manuscript. All authors have participated sufficiently in the work and agreed to be accountable for all aspects of the work.

Ethics Approval and Consent to Participate

The Institutional Animal Care and Animal Ethics Committee of Lanzhou University Second Hospital authorized all experimental animal operations and sample collection (approval number: D2021-051).

Acknowledgment

We would like to thank all the participants for their contributions and the reviewers for their constructive comments.

Funding

This research was funded by the National Natural Science Foundation of China (Grant number 82160840), Cuiying Scientific and Technological Innovation Program of Lanzhou University Second Hospital (Grant number CY2023-QN-B11), and Gansu Province Science Foundation for Youths (Grant number 23JRRA1007).

Conflict of Interest

The authors declare no conflict of interest.

References

[1] Morris G, O'Brien D, Henshall DC. Opportunities and challenges for microRNA-targeting therapeutics for epilepsy. Trends in Pharmacological Sciences. 2021; 42: 605–616.

[2] Thijs RD, Surges R, O'Brien TJ, Sander JW. Epilepsy in adults. Lancet. 2019; 393: 689–701.

[3] Hakami T. Neuropharmacology of Antiseizure Drugs. Neuropsychopharmacology Reports. 2021; 41: 336–351.

[4] Vezzani A, Ravizza T, Bedner P, Aronica E, Steinhäuser C, Boison D. Astrocytes in the initiation and progression of epilepsy. Nature Reviews. Neurology. 2022; 18: 707–722.

[5] Rana A, Musto AE. The role of inflammation in the development of epilepsy. Journal of Neuroinflammation. 2018; 15: 144.

[6] Vezzani A, Balosso S, Ravizza T. Neuroinflammatory pathways as treatment targets and biomarkers in epilepsy. Nature Reviews. Neurology. 2019; 15: 459–472.

[7] Almeida C, Pongilio RP, Móvio MI, Higa GSV, Resende RR, Jiang J, *et al*. Distinct Cell-specific Roles of NOX2 and MyD88 in Epileptogenesis. Frontiers in Cell and Developmental Biology. 2022; 10: 926776.

[8] Wang G, Zhu Z, Xu D, Sun L. Advances in Understanding CREB Signaling-Mediated Regulation of the Pathogenesis and Progression of Epilepsy. Clinical Neurology and Neurosurgery. 2020; 196: 106018.

[9] Tian XH, Wu JH. Tanshinone derivatives: a patent review (January 2006 - September 2012). Expert Opinion on Therapeutic Patents. 2013; 23: 19–29.

[10] Subedi L, Gaire BP. Tanshinone IIA: A phytochemical as a promising drug candidate for neurodegenerative diseases. Pharmacological Research. 2021; 169: 105661.

[11] Wang J, Kong L, Guo RB, He SY, Liu XZ, Zhang L, *et al*. Multifunctional icariin and tanshinone IIA co-delivery liposomes with potential application for Alzheimer's disease. Drug Delivery. 2022; 29: 1648–1662.

[12] Lin L, Jadoon SS, Liu SZ, Zhang RY, Li F, Zhang MY, *et al*. Tanshinone IIA Ameliorates Spatial Learning and Memory Deficits by Inhibiting the Activity of ERK and GSK-3β. Journal of Geriatric Psychiatry and Neurology. 2019; 32: 152–163.

[13] Ma H, Hu ZC, Long Y, Cheng LC, Zhao CY, Shao MK. Tanshinone IIA Microemulsion Protects against Cerebral Ischemia Reperfusion Injury via Regulating H3K18ac and H4K8ac *In Vivo* and *In Vitro*. The American Journal of Chinese Medicine. 2022; 50: 1845–1868.

[14] Li ZH, Cheng L, Wen C, Ding L, You QY, Zhang SB. Activation of CNR1/PI3K/AKT Pathway by Tanshinone IIA Protects Hippocampal Neurons and Ameliorates Sleep Deprivation-Induced Cognitive Dysfunction in Rats. Frontiers in Pharmacology. 2022; 13: 823732.

[15] Jia C, Zhang R, Wei L, Xie J, Zhou S, Yin W, *et al*. Investigation of the mechanism of tanshinone IIA to improve cognitive function via synaptic plasticity in epileptic rats. Pharmaceutical Biology. 2023; 61: 100–110.

[16] Magee JC, Grienberger C. Synaptic Plasticity Forms and Functions. Annual Review of Neuroscience. 2020; 43: 95–117.

[17] Pototskiy E, Dellinger JR, Bumgarner S, Patel J, Sherrerd-Smith W, Musto AE. Brain injuries can set up an epileptogenic neuronal network. Neuroscience and Biobehavioral Reviews. 2021; 129: 351–366.

[18] Wang Y, Fu AKY, Ip NY. Instructive roles of astrocytes in hippocampal synaptic plasticity: neuronal activity-dependent regulatory mechanisms. The FEBS Journal. 2022; 289: 2202–2218.

[19] Martella G, Bonsi P, Johnson SW, Quartarone A. Synaptic Plasticity Changes: Hallmark for Neurological and Psychiatric Disorders. Neural Plasticity. 2018; 2018: 9230704.

[20] Ribak CE, Tran PH, Spigelman I, Okazaki MM, Nadler JV. Sta-

tus epilepticus-induced hilar basal dendrites on rodent granule cells contribute to recurrent excitatory circuitry. The Journal of Comparative Neurology. 2000; 428: 240–253.
[21] Colella R, Lu C, Hodges B, Wilkey DW, Roisen FJ. GM1 enhances the association of neuron-specific MAP2 with actin in MAP2-transfected 3T3 cells. Brain Research. Developmental Brain Research. 2000; 121: 1–9.
[22] Cao HY, Jiang YW, Liu ZW, Wu XR. Effect of recurrent epileptiform discharges induced by magnesium-free treatment on developing cortical neurons in vitro. Brain Research. Developmental Brain Research. 2003; 142: 1–6.
[23] Mangan PS, Kapur J. Factors underlying bursting behavior in a network of cultured hippocampal neurons exposed to zero magnesium. Journal of Neurophysiology. 2004; 91: 946–957.
[24] Mele M, Vieira R, Correia B, De Luca P, Duarte FV, Pinheiro PS, *et al*. Transient incubation of cultured hippocampal neurons in the absence of magnesium induces rhythmic and synchronized epileptiform-like activity. Scientific Reports. 2021; 11: 11374.
[25] Bengzon J, Mohapel P, Ekdahl CT, Lindvall O. Neuronal apoptosis after brief and prolonged seizures. Progress in Brain Research. 2002; 135: 111–119.
[26] Jiang ZM, Qiu HB, Wang SQ, Guo J, Yang ZW, Zhou SB. Ganoderic acid A potentiates the antioxidant effect and protection of mitochondrial membranes and reduces the apoptosis rate in primary hippocampal neurons in magnesium free medium. Die Pharmazie. 2018; 73: 87–91.
[27] Mateos-Aparicio P, Rodríguez-Moreno A. Calcium Dynamics and Synaptic Plasticity. Advances in Experimental Medicine and Biology. 2020; 1131: 965–984.
[28] Diering GH, Huganir RL. The AMPA Receptor Code of Synaptic Plasticity. Neuron. 2018; 100: 314–329.
[29] Voglewede MM, Zhang H. Polarity proteins: Shaping dendritic spines and memory. Developmental Biology. 2022; 488: 68–73.
[30] Chidambaram SB, Rathipriya AG, Bolla SR, Bhat A, Ray B, Mahalakshmi AM, *et al*. Dendritic spines: Revisiting the physiological role. Progress in Neuro-Psychopharmacology & Biological Psychiatry. 2019; 92: 161–193.
[31] Jean G, Carton J, Haq K, Musto AE. The role of dendritic spines in epileptogenesis. Frontiers in Cellular Neuroscience. 2023; 17: 1173694.
[32] Zagrebelsky M, Holz A, Dechant G, Barde YA, Bonhoeffer T, Korte M. The p75 neurotrophin receptor negatively modulates dendrite complexity and spine density in hippocampal neurons. The Journal of Neuroscience. 2005; 25: 9989–9999.
[33] Kanjhan R, Noakes PG, Bellingham MC. Emerging Roles of Filopodia and Dendritic Spines in Motoneuron Plasticity during Development and Disease. Neural Plasticity. 2016; 2016: 3423267.
[34] Grintsevich EE. Effects of neuronal drebrin on actin dynamics. Biochemical Society Transactions. 2021; 49: 685–692.
[35] Kowiański P, Lietzau G, Czuba E, Waśkow M, Steliga A, Moryś J. BDNF: A Key Factor with Multipotent Impact on Brain Signaling and Synaptic Plasticity. Cellular and Molecular Neurobiology. 2018; 38: 579–593.
[36] Kinjo ER, Rodríguez PXR, Dos Santos BA, Higa GSV, Ferraz MSA, Schmeltzer C, *et al*. New Insights on Temporal Lobe Epilepsy Based on Plasticity-Related Network Changes and High-Order Statistics. Molecular Neurobiology. 2018; 55: 3990–3998.
[37] Li C, Ke C, Su Y, Wan C. Exercise Intervention Promotes the Growth of Synapses and Regulates Neuroplasticity in Rats With Ischemic Stroke Through Exosomes. Frontiers in Neurology. 2021; 12: 752595.
[38] Han T, Qin Y, Mou C, Wang M, Jiang M, Liu B. Seizure induced synaptic plasticity alteration in hippocampus is mediated by IL-1β receptor through PI3K/Akt pathway. American Journal of Translational Research. 2016; 8: 4499–4509.
[39] Liu AH, Chu M, Wang YP. Up-Regulation of Trem2 Inhibits Hippocampal Neuronal Apoptosis and Alleviates Oxidative Stress in Epilepsy via the PI3K/Akt Pathway in Mice. Neuroscience Bulletin. 2019; 35: 471–485.